Cement and Concrete Research 95 (2017) 1–8

Contents lists available at ScienceDirect

Cement and Concrete Research

journal homepage: www.elsevier.com/locate/cemconres

Insights into delayed ettringite formation damage through acoustic nonlinearity

Mehdi Rashidi [a], Alvaro Paul [b], Jin-Yeon Kim [a,c], Laurence J. Jacobs [a,c], Kimberly E. Kurtis [a,*]

[a] School of Civil and Environmental Engineering, Georgia Institute of Technology, Atlanta, GA 30332-0355, United States
[b] Facultad de Ingeniería y Ciencias Aplicadas, Universidad de los Andes, Chile
[c] G. W. Woodruff School of Mechanical Engineering, Georgia Institute of Technology, Atlanta, GA 30332-0405, United States

ARTICLE INFO

Article history:
Received 13 October 2016
Received in revised form 9 February 2017
Accepted 10 February 2017
Available online 20 February 2017

Keywords:
Delayed ettringite formation (DEF) (C)
Microcracking (B)
Expansion (C)
Thermal treatment (A)
Nonlinear acoustics

ABSTRACT

A nonlinear acoustic approach for the detection and quantification of damage in mortars affected by delayed ettringite formation (DEF) is used to provide insights into the degradation mechanism at the microscale and its correlation with bulk expansion. The nonlinear acoustic technique, Nonlinear Impact Resonance Acoustic Spectroscopy (NIRAS) successfully differentiates among mortars experiencing various amounts of expansion and microstructurally-evident distress due to DEF. Results indicate that mortars are damaged both during the early-age high-temperature curing and subsequent 23 °C-limewater curing. However, the time of initiation of expansion occurs earlier for samples showing higher damage level (as measured by average nonlinearity parameter) at the end of high-temperature curing. During the exposure period, the ratio of absolute maximum to the initial average nonlinearity parameter of DEF-affected mortars varies from 3 to 30, indicating that the DEF damage can increase more than an order of magnitude greater than that experienced during the high-temperature curing.

1. Introduction

Delayed ettringite formation (DEF) is most often associated with the later formation of ettringite within concrete or mortar exposed to high temperatures during early stages of cement hydration and can lead to expansion, cracking, and loss of mechanical properties and durability in cement-based materials. DEF has been noted in precast concrete when steam and high-temperature curing are used, and in mass concrete elements, where the evolved heat during cement hydration can result in high internal temperatures if improperly designed [1–4].

While DEF has been identified as a deleterious expansive chemical reaction in cement-based materials, the underlying mechanism of expansion remains a subject of ongoing examination. However, it is generally accepted that i) occurrence of DEF requires an early-age curing temperature of higher than 70 °C, ii) cement/binder chemistry determines the amount of ettringite formed initially during hydration and later due to DEF, and iii) the developed stresses depend on the microstructure of the affected material [5]. DEF-related expansion is most commonly attributed to the expansive pressures caused by the formation of ettringite under supersaturation in confined nanopores within cement paste. The pressure can cause expansion, microcracking, and contribute to the degradation of cement-based composites [6,7]. It is generally accepted that the larger crystals of secondary ettringite precipitating in existing voids, cracks, and interfacial transition zone (ITZ) gaps do not contribute to the DEF-related expansion and damage.

The relationship between ettringite formation, expansion, and damage in DEF-affected cement-based materials is not well understood. Although, thermodynamic analysis [7] and finite element (FE) modeling [8] have been performed to better understand the degradation of cement-based materials during DEF development, no general relationship between the increase in the ettringite content, DEF-related expansion, and damage has been developed [5]. To investigate the correlation between expansion and microscale damage caused by DEF, a nondestructive acoustic approach is used. In contrast to the destructive approaches, nondestructive acoustic techniques can be applied to the same expanding samples periodically to provide temporal information about the damage accumulation by DEF. However, various nondestructive techniques exhibit various sensitivity levels to damage. For instance, while the macro-behavior of cement-based materials can be monitored using linear acoustic techniques such as dynamic elastic modulus, the progression of microcracking in those materials is better monitored by nonlinear acoustic techniques such as nonlinear acoustic resonance techniques. Compared to linear acoustic techniques, nonlinear resonance techniques are generally more sensitive to microcracks. For example, the ratio of increase in material hysteresis nonlinearity to decrease in the dynamic elastic modulus of specimen may exceed two orders of magnitude [9]. The high sensitivity of nonlinear acoustic techniques to the presence of microcracks makes them advantageous for the assessment of damage in cement-based materials due to thermal

* Corresponding author.
E-mail address: kimberly.kurtis@ce.gatech.edu (K.E. Kurtis).

http://dx.doi.org/10.1016/j.cemconres.2017.02.004
0008-8846/

effects [10], ASR [9,11–13], and drying shrinkage [14], as well as the detection of microcrack filling during carbonation [15]. Here, a nonlinear acoustic resonance technique, Nonlinear Impact Resonance Acoustic Spectroscopy (NIRAS), is used for the assessment of the DEF damage evolution.

This quantitative study characterizes the damage in heat-affected mortars at the microscale and examines the relationship between microcracking development (measured as nonlinearity) and expansion. The source of the microstructural damage is further confirmed by variable pressure scanning electron microscopy (VP-SEM) with energy dispersive X-ray spectroscopy (EDS) microanalysis. Relating the results from NIRAS measurements, expansion and microscopy provides new insights relating microscale damage and expansion during progressive DEF.

2. Methodology

2.1. Materials and sample preparation

In total, five commercially available cements were examined, with a range of compositions to assess varying degrees and rates of damage by DEF. Mortars were prepared from three ASTM C150 Type I cements (labeled as Type I-A, Type I-B, and Type I-C cement), one ASTM C150 Type V cement, and one ASTM C150 Type III cement. The Type V and Type III cements were selected to represent cases of relatively low and high susceptibility to DEF [16], while three compositions of Type I cement provide a range of sulfate, alumina, and C_3A contents (Table 1). Furthermore, all cements are classified as low-alkali cements according to ASTM C150.

Natural siliceous sand (specific gravity = 2.66 and fineness modulus = 2.43) was obtained from an alluvial/marine deposit in Georgia. X-ray diffraction analysis indicated that the sand is mainly quartz. Furthermore, sand particles vary in morphology and surface texture, but are primarily weathered angular particles (Fig. 1).

Mortar was prepared following the proportions of cement and natural siliceous sand given in ASTM C1038, and the mixing procedure given in ASTM C305. The water-to-cement mass ratio (w/c) was 0.50 and a sand-to-cement mass ratio (s/c) was 2.75.

2.2. Exposure and expansion measurements

Ten 25 × 25 × 285-mm prismatic mortar bars were cast for each cement. Two curing conditions were used in the first 24 h: half of the specimens were kept in sealed containers at 23 ± 1.5 °C and served as controls, and the other half were exposed to the Kelham high-temperature curing cycle (Fig. 2) which is commonly used for examining the potential for DEF [16–18]. Subsequently, all mortars were cured in limewater baths at 23 ± 1.5 °C, with samples prepared from each cement cured separately.

The length of mortar bars was measured periodically using a comparator conforming ASTM C490 standard. It should be noted that, although no expansion limit has been defined for a deleterious DEF-expansion, 0.1% expansion limit is often considered as an expansion limit for mortar bars [19–21].

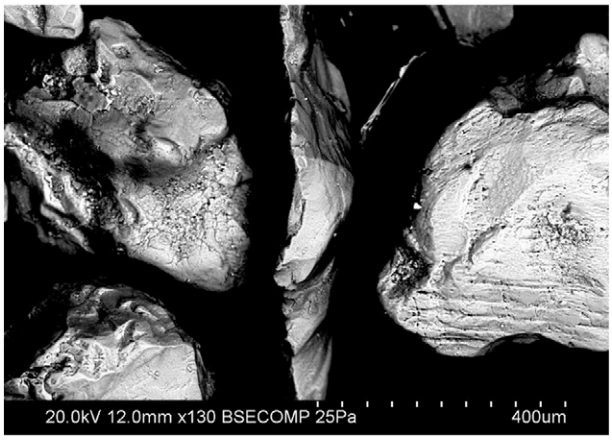

Fig. 1. Natural siliceous sand particles at 130x magnification.

2.3. Microscopy

To inspect microstructure and assess damage in heat-cured specimens, microscopy samples were obtained from mortar bars at the later ages of limewater storage. Sections were cut using an ethanol-cooled diamond saw at a slow speed (30 rotations per minute) to minimize the introduction of artifacts. After gently wiping the surfaces with ethanol, samples were stored in sealed containers. This sample preparation procedure was designed to preserve the original condition of the bars as much as possible. Then, samples were analyzed within 2 h of preparation using a Hitachi S-3700N Variable Pressure Scanning Electron Microscope (VP-SEM) at 25 Pa and 30 kV with EDS microanalysis capabilities.

2.4. NIRAS measurements

NIRAS measurements were performed as has been previously described [9,12,23,24]. Briefly, these are accomplished by the application of light impacts of increasing amplitude to the mid-length of a mortar bar, and the acquisition of the time domain signal using an accelerometer located at the end of the bar (Fig. 3). Then, the time domain signals are transformed into the frequency domain using the fast Fourier transform (FFT) and the hysteresis nonlinearity parameter (α') is

Table 1
Oxide analysis and Bogue potential composition of cements.

Cement type	Oxide analysis								SO_3/Al_2O_3
	SiO_2	Al_2O_3	Fe_2O_3	CaO	MgO	$(Na_2O)_e$	SO_3	LOI	
Type I-A	19.78	4.61	3.37	62.75	3.07	0.49	2.55	2.57	0.70
Type I-B	19.58	4.79	3.38	64.20	1.06	0.49	3.26	2.61	0.87
Type I-C	19.40	5.48	3.33	63.83	0.79	0.53	3.18	1.64	0.74
Type III	19.81	5.52	3.31	63.99	0.79	0.47	4.14	1.67	0.96
Type V	21.10	3.95	4.42	62.49	3.05	0.44	2.35	1.33	0.76

Cement type	Bogue potential composition				Blaine fineness m^2/kg
	C_3S	C_2S	C_3A	C_4AF	
Type I-A	62.08%	9.89%	6.50%	10.26%	393
Type I-B	66.26%	6.15%	6.97%	10.28%	413
Type I-C	61.76%	9.03%	8.88%	10.14%	401
Type III	56.34%	14.29%	9.03%	10.06%	498
Type V	54.50%	19.38%	2.97%	13.45%	376

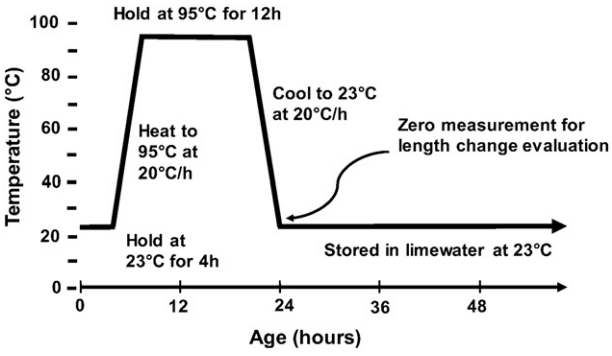

Fig. 2. Kelham high-temperature curing cycle (modified from [22]).